



Contents lists available at ScienceDirect

## Physics Letters A

www.elsevier.com/locate/pla



## Stretching and folding mechanism in foams

Alberto Tufaile\*, Adriana Pedrosa Biscaia Tufaile

Escola de Artes, Ciências e Humanidades, Soft Matter Laboratory, Universidade de São Paulo, 03828-000 São Paulo, SP, Brazil

## ARTICLE INFO

## Article history:

Received 19 May 2008

Received in revised form 10 August 2008

Accepted 28 August 2008

Available online 2 September 2008

Communicated by A.R. Bishop

## PACS:

05.45.-a

47.57.Bc

47.53.+n

## Keywords:

Foams

Chaos

Logistic growth

Baker map

## ABSTRACT

We have described the stretching and folding of foams in a vertical Hele–Shaw cell containing air and a surfactant solution, from a sequence of upside-down flips. Besides the fractal dimension of the foam, we have observed the logistic growth for the soap film length. The stretching and folding mechanism is present during the foam formation, and this mechanism is observed even after the foam has reached its respective maximum fractal dimension. Observing the motion of bubbles inside the foam, large bubbles present power spectrum associated with random walk motion in both directions, while the small bubbles are scattered like balls in a Galton board.

© 2008 Published by Elsevier B.V.

When a liquid containing a surfactant is shaken in the presence of air, a foam is formed by the action of deformation and stretching of the air/liquid interface. If this foam is left to rest, the interface evolves towards a minimal surface by a minimization process of energy. If the motion persists, the liquid flows through the interstitial spaces between bubbles, along with the rearrangement of the foam structure. We consider the following question: what are the descriptions from the point of view of dynamical systems theory applicable to the complex spatio-temporal behavior of the foam evolution? The study of chaotic systems turns out to be useful for analyzing the evolution of the foam structure [1], and the connections between chaos and foams should be explored. One possible connection is related to the process of mixing of the interface between liquid and air, suggesting the occurrence of some kind of stretching and folding mechanism [2], like those observed in the iterations of a two-dimensional map known as baker map.

The vast literature on foams and their evolution suggests the complexity of the involved phenomena [3,4]. Some works have addressed the foaming dynamics from a series of upside-down flips in a device in which a foam is confined between two parallel plates, known as Hele–Shaw cell [5,6] unveiling the temporal evolution of the number of bubbles by a kinematic model, which

depends on some parameters, such as the area of the cell, the initial liquid content, the characteristic length of the bubbles, and the bubble split rate. We are presenting the signature of the stretching and folding mechanism in a foam, obtained during a sequence of flips in a vertical Hele–Shaw cell partially filled with a surfactant. We also compared this foam evolution to a sequence of iterations obtained from the baker map [2], in which the stretching and folding mechanism is present.

Our experiments of foam formation were performed in a transparent Hele–Shaw cell, consisting of two plain parallel plexiglass plates separated by a narrow gap ( $20 \times 20 \times 0.2 \text{ cm}^3$ ), filled with surfactant solution and air, at room temperature. The cell is flipped upside-down in order to observe the foam formation. A close-up of foam is shown in Fig. 1(a). After each flip, the cell is left at rest for a relaxation time of 600 s. An amount of a commercial dishwashing liquid ( $V = 8 \text{ cm}^3$ ), manufactured by Bombril, is used without dilution. The essential surfactant is Linear Alkylbenzene Sulfonate (LAS). The surface tension is  $\gamma = 25 \text{ dyne/cm}$  obtained by the ring method, and the density of this detergent is  $\rho = 0.95 \text{ g/cm}^3$ . Each flip of the Hele–Shaw cell is referred in this Letter as iteration, and  $nf$  is the number of successive iterations. The photographs of the foam were recorded with a digital camera with a resolution of 6.0 megapixel. The images were processed, converted into binary images, as it is shown in Fig. 1(b), and analyzed in a personal computer, leading to accuracy up to 0.2 mm. With these images we have estimated the total length of the soap film ( $L$ ), and obtained the series of lengths  $\{L_{nf}\}$ .

\* Corresponding author.

E-mail address: tufaile@usp.br (A. Tufaile).

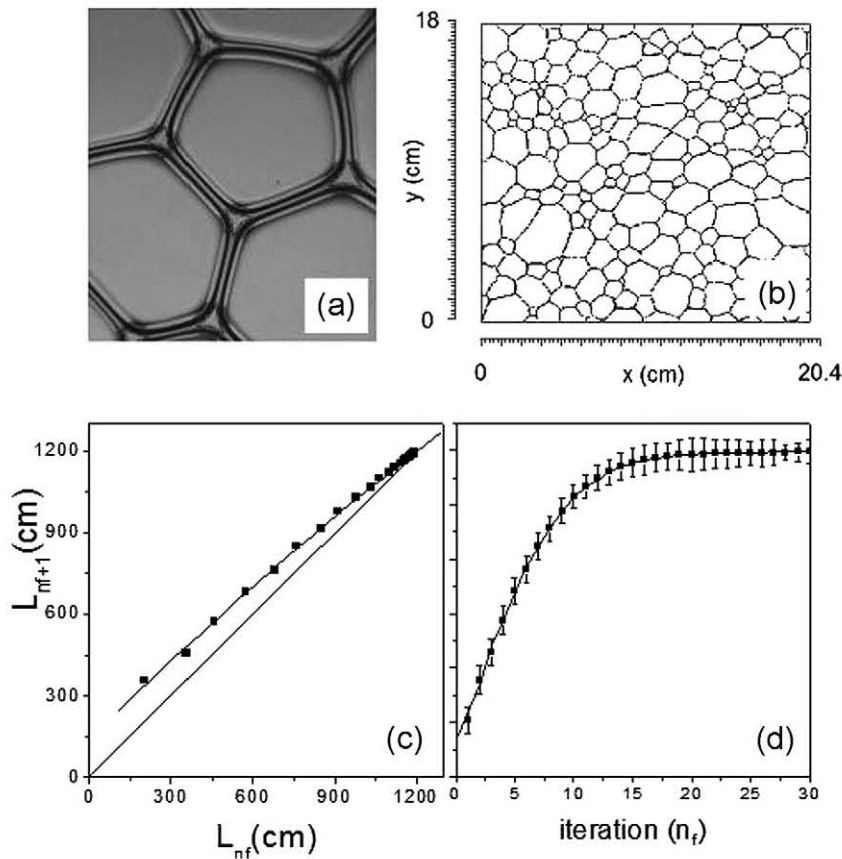


**Fig. 1.** (a) A close-up of a foam in the Hele-Shaw cell, showing the liquid elements of this foam during the drainage. The binary image of a foam capturing the skeleton of an arrangement of the soap film is shown in (b). The reconstructed first return map of the film length  $L_{nf}$  in (c) shows that a non-linear map can be obtained with a parabola fit. The values obtained using this parabola fit are represented in the continuous curve superposed to the experimental points in (d), showing that for a sequence of iterations the film length  $L_{nf}$  is associated with a logistic growth.

In each iteration we followed the development of a planar network of filaments extending through-out the Hele-Shaw cell, with movements forced by the drainage of the liquid along the films and the parallel plates of the cell, following the principles of balancing forces and minimization of energy. After the relaxation time for the first iteration, the total soap film length reaches 200 cm. In the second iteration, the liquid is drained through this irregular foam. The length of the film after the relaxation process for this second iteration is around 355 cm. We have obtained that the total length of the interfaces between bubbles as a function of the number of iterations  $nf$  is bounded. The limiting value is around 1240 cm. After this limit, even if the liquid and the air that form the foam are displaced by the act of flipping, for further iterations the system tends to a stable dynamical length. In order to give some hint of the underlying process involved and to characterize this behavior, we have obtained the total film length  $L_{nf}$ , and plotted its first return map ( $L_{nf+1}$  vs.  $L_{nf}$ ) [7] in Fig. 1(c), along with the straight line  $L_{nf+1} = L_{nf}$ . By inspection of the distribution of these values, the successive values of  $L_{nf}$  can be reduced to a low order map. The fit of a parabola is:

$$L_{nf+1} = a_1 + b_1 L_{nf} + c_1 L_{nf}^2, \quad (1)$$

with the fitting parameters  $a_1 = 138$ ,  $b_1 = 0.99$  and  $c_1 = -0.00009$ . The sequence of values of  $L_{nf}$ , which are generated by the map, converges to a fixed point, represented by the intersection of the straight line with the parabolic function. The iterations obtained from this map are shown as a continuous curve superposed to the experimental points in Fig. 1(d). The agreement of this curve and the experimental data reveals that the evolution of the film length  $L_{nf}$  can be characterized as the logistic growth [8], from

the point of view of dynamical systems. With this length we can estimate the ratio between the stored energy in the complete developed foam and the total energy input. The energy stored in the dry foam  $E_{foam}$  is proportional to the soap film length, the distance between parallel plates  $d$ , and the surface tension  $\gamma$ , there is a factor 2 due to the two air-liquid interfaces, so that the energy tends to  $E_{foam} = 2d\gamma L_{nf}$ . Consequently the energy stored in this dry foam grows with the number of iterations up to  $E_{foam} = 1.2$  mJ. Considering the energy released by the liquid for each flip as  $E_f = \rho Vgh = 17$  mJ, where  $h = 18$  cm, and  $g$  is the gravity acceleration, for twenty iterations, the total energy input is around 0.3 J. The stored energy is the order of one thousandth of the total energy input.

In order to follow the existence of spatial divergence in the experimental system, the trajectories of four tiny bubbles were observed. These bubbles were aligned in a space of 1 cm, each one being around 0.2 mm in diameter. When the cell was flipped, these bubbles were photographed, and a typical sequence is shown in Fig. 2, showing the transient evolution of four bubbles in the same iteration. The stretching factor is qualitatively observed for this case along the vertical axis, while they almost superpose themselves at the horizontal axis, with the fold process in this direction. This motion indicates the presence of stretching and folding mechanism, which would give a positive Lyapunov exponent, as observed in a flowing fluid using minute particles coated with fluorescent dye [9].

The logistic dynamics of Eq. (1) limits the film length  $L$  such that the system approaches statistically to a self-similar state. In general, foams are not perfectly self-similar or fractals, due to finite size of Hele-Shaw cell and the minimum size of bubbles.

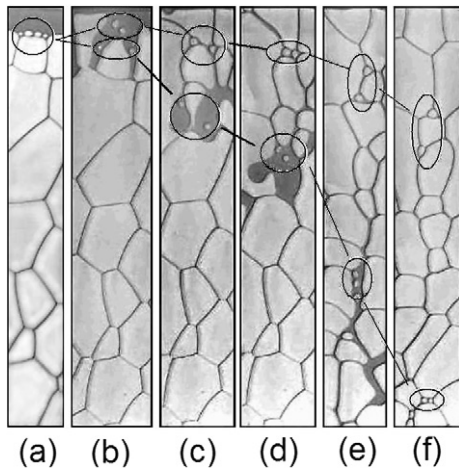


**Fig. 2.** Photographs of a sequence illustrating the stretching and folding mechanism in the Hele-Shaw cell, for  $nf = 5$ . Four neighbor bubbles aligned at the interface of the liquid and the foam. The distance between the center of the first and the fourth bubble is 1 cm in (a). The drainage of the liquid starts to change the position of these bubbles, as the cell is flipped in (b), enabling us to follow the evolution of some constituents of the foam. In (c) two bubbles of the initial group of tiny bubbles remained attached to the network of films at the top, while two bubbles fall continually with the liquid. In (d) while the fall of the liquid changes the configuration of the foam transporting the two tiny bubbles, the two bubbles left at the top of the cell move slowly, following the edges of larger bubbles. The two bubbles at the top barely move, and the two bubbles at bottom side are entrained by the liquid flow in (e), scattered by the bubble edges formed in the previous iteration. The final position of the four bubbles is shown in (f), in which the distance between bubbles was stretched by 9 cm in the vertical axis, while these same bubbles are overlapped in the horizontal axis, folding the distance between them in this direction.

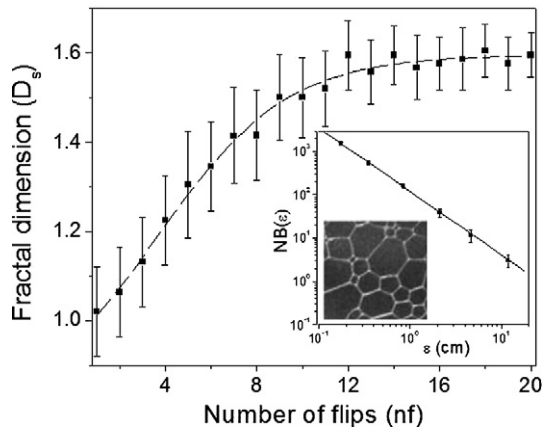


**Fig. 3.** In the main plot, it is shown the fractal dimension  $D_s$  of foams obtained from a sequence of flips  $nf$  from 1 to 20. The dashed line is a non-linear fitting to these data showing the same behavior of the film length evolution of the logistic growth. In the inset the plot of the box counting function  $NB(\epsilon)$  with  $D_s = 1.48$ , with a photograph of a detail of the measured foam with area equal to  $1 \text{ cm}^2$ .

Nonetheless a macroscopic scale law can be found using the concept of fractal dimension [10]. Thus a dimension estimate involves a nontrivial extrapolation from a finite data set to a distribution of the liquid filaments of the foam. The fractal analysis was applied over the cross section of the foam in the Hele-Shaw cell. To measure the dimension  $D_s$  of the foam, we have applied the box counting method [10]. The estimates for the fractal dimension for a sequence of iterations are shown in Fig. 3, ranging from 1.0 to 1.6. A nonlinear fitting to the experimental data of the dimension values indicates a similar behavior obtained as for the case of the film length  $L_{nf}$ . This result shows proportionality between the different variables of the system: the film length  $L$  and the fractal dimension  $D_s$  of the foam.

Some interesting properties observed in these foams evoke some idealized models from the theory of chaotic systems. These properties reflect the evolution observed in the foam, such as the emergence of spatial expansion of structured fluids. A very simple dynamical model showing the spatial evolution is the baker map [2]. This model illustrates how a stretching in one direction can work together, with compression and folding in another direction to produce deterministic chaos. After every time step the unit square is first squeezed vertically ( $y$ ), and stretched horizontally ( $x$ ), subsequently, it is cut into pieces of unit width that are placed at the top of each other. The equations of the map are:

$$B(x, y) = \begin{cases} (2x + \beta y, \frac{y}{2}) & \text{for } 0 \leq x < 0.5, \\ (2x - 1 + \beta y, 1 + \frac{y-1}{2}) & \text{for } 0.5 \leq x < 1. \end{cases} \quad (2)$$

In order to control the global behavior of this map, we have used the parameter  $\beta$  as the unidirectional coupling between the variables  $x$  and  $y$ . We have obtained a sequence of time series, with 12 000 points each one, discarding a transient of 10 000 iterations, in the interval  $10^{-6} < \beta < 10^{-5}$ . The baker map presents two Lyapunov exponents in this interval: a positive one  $\lambda_1$ , and a negative one  $\lambda_2$ , characterizing the dynamics of this system as chaotic. There is a relation between the Lyapunov exponents and the fractal dimension of the chaotic behavior, known as the Lyapunov dimension  $D_l$ , and in the case of two-dimensional maps with  $\lambda_1 > 0 > \lambda_2$  and  $\lambda_1 + \lambda_2 < 0$  is given by [7]:

$$D_l = 1 + \frac{\lambda_1}{|\lambda_2|}. \quad (3)$$

For  $\beta = \beta_1 = 4.5 \times 10^{-6}$ , we have obtained the value of dimension closer to the value of dimension obtained for the experiment, with  $D_s = 1.6$  ( $nf > 20$ ).

The importance of this model is in its utility to bring some findings about the general evolution of the foam. It is therefore interesting to compare the dynamical properties between this map and the experiment with a foam completely developed. In Fig. 4(a), we exemplified the time series of the coordinate  $y$  obtained from the baker map using the coupling constant  $\beta_1$ . In the experiment, this is done in two steps: first, we performed a sequence of thirty flips ( $nf = 30$ ), obtaining a fully developed foam, and after that we recorded the normalized coordinates  $(x, y)$  of the geometrical center of some chosen bubbles from  $nf = 31$  to 70. The time series of the vertical position for bubble diameters of 5 mm and 1 mm are shown in Figs. 4(b) and 4(c), respectively. Qualitatively, we can observe that the amplitude of motion of the baker map is very large, while the amplitude of bubble motion is size sensitive. The difference of behavior between these two bubbles is related to the bubble size segregation, in which was stated that at the beginning of the experiment, the large bubbles have been observed mainly at the center of the cell, while small bubbles have been seen at the top and the bottom.

A way to characterize the dynamical behavior of a time series is to apply the power spectrum method [11]. Using the Fast Fourier Transform (FFT), we have obtained the power spectrum for the time series of each variable  $(x, y)$  of the baker map with the constant  $\beta_1$ , for different values of the initial conditions. The spectrum of the baker map in Fig. 4(d) presents a broad band, with the same decay for both variables  $x$  and  $y$  with  $f^{-\alpha}$  ( $\alpha = 0.7$ ). We also have obtained numerically the spectra observed in some dynamical systems, such as the Galton board dynamics, in which collisions of a particle with scatterers can be modeled by a map obtained from Ref. [2]:

$$f(y) \equiv \begin{cases} y + 1 & \text{for } y < 0, \\ \frac{y-(m-1)}{r} + (m-1-\Delta) & \text{for } (m-1) < y < (m-r), \\ \frac{y-m}{r} + (m+\Delta) & \text{for } (m-r) < y < m, \\ y - 1 & \text{for } (N+1) < y, \end{cases} \quad (4)$$

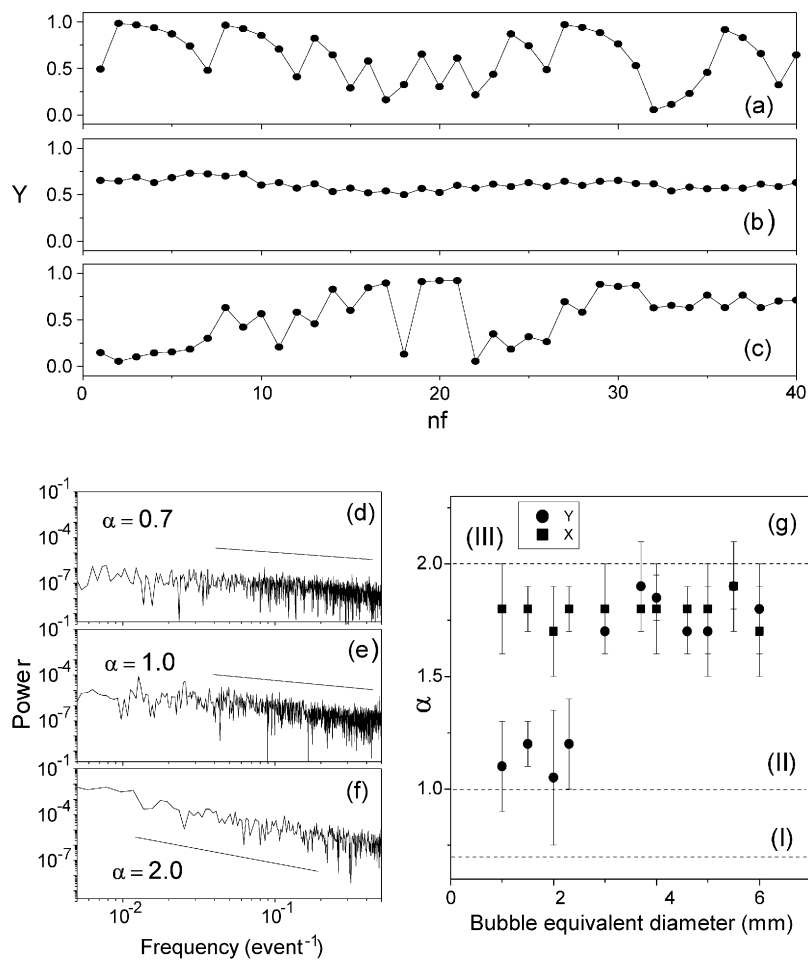


**Fig. 4.** The time series of the coordinate  $y$  obtained from the baker map in (a), using the coupling constant  $\beta_1$ . The time series of the normalized coordinate of the vertical position for a bubble diameter of 5 mm is shown in (b), and in (c) the time series of a bubble diameter of 1 mm. The power spectra for the time series of variable  $y$  with the decay like  $f^{-\alpha}$  of some systems are shown in (d)–(f). In (d) the baker map with the constant  $\beta_1$ , presenting a broad band, with  $\alpha = 0.7$ . In (e) the power spectrum of the Galton board dynamics, with  $\alpha = 1.0$ , and the power spectrum for the random walk is shown in (f) with  $\alpha$  close to 2.0. We have applied the same method to obtain the power spectra of the bubble motion for the coordinates ( $x$ ,  $y$ ) of some bubbles and obtained their respective  $\alpha$  values shown in (g). The dashed lines in (g) indicate the values of  $\alpha$  for the baker map in (I), for the Galton board dynamics in (II), and for the random walk in (III).

where  $m = 0, \dots, N + 1$ ,  $\Delta = 1$ ,  $N = 8$ , and  $l + r = 1$ , with  $l = 1/2$  for unbiased collisions. From this map we have obtained a spectrum with  $\alpha = 1.0$  shown in Fig. 4(e), and it also presents the stretching and folding mechanism. The spectrum for the case of the traditional random walk is shown in Fig. 4(f), with  $\alpha$  close to 2, illustrates the upper limit for  $\alpha$  values.

We have applied the same method for the experimental data for the position of different bubble sizes, ranging from 1 mm to 6 mm for  $31 < nf < 70$ , as it is shown in Fig. 4(g). We have observed basically two different behaviors of bubble motion, one associated with Galton board dynamics for bubble diameter up to 2.3 mm, and another one associated with random walk for bubble diameter higher than 2.3 mm. The difference between the motions of these two ranges of bubble size can be explained by the fact that small bubbles have the tendency of being dragged by a drop falling during the liquid drainage, and consequently traveling large distances in the vertical direction. In addition to this, they can be scattered by large bubbles, mimicking the spectrum of the Galton board dynamics, and this result gives us an idea of the process behind the bubble motion of these small bubbles in the vertical direction. On the other hand, large bubbles have the tendency of being displaced by short distances in both directions in each step, similar to the displacement observed in the random walk. In this way, when the foam is completely developed, there is a structure

formed by large bubbles scattering the liquid transporting small bubbles.

In conclusion, we have described the stretching and folding mechanism present in foams obtained from a Hele–Shaw cell containing liquid detergent and air, for a sequence of upside-down flips. Based on the experimental data from the series of foam lengths, it was found that the foam length has reached a maximum value as a function of the number of flips, following the logistic growth. During this stage, we also have found the existence of spatial divergence in the foam elements following neighbor bubbles, in which the distance between bubbles was stretched in the vertical axis, while in the horizontal the distance was folded. After that, we have studied the baker map, which presents the stretching and folding mechanism, controlled by a coupling parameter, such that we were able to compute the Lyapunov exponents, and its respective fractal dimension. The baker map has motivated us to compare the dynamical behavior of the bubble motion for a sequence of iterations using the power spectrum method. The stretching and folding mechanism is present during the foam formation, and this mechanism is observed even after the foam has reached its respective maximum fractal dimension. Large bubbles present power spectrum associated with random walk motion in both directions, while the small bubbles behave in the same way in the horizontal direction, but are scattered like balls in a Galton board in the vertical direction.

### Acknowledgements

This work was supported by Conselho Nacional de Desenvolvimento Científico e Tecnológico (CNPq), and Instituto do Milênio de Fluidos Complexos. We thank Fábria Almeida Lino and Luana Matias for their assistance.

### References

- [1] A. Tufaile, J.C. Sartorelli, P. Jeandet, G. Liger-Belair, *Phys. Rev. E* 75 (2007) 066216.
- [2] J. Vollmer, *Phys. Rep.* 372 (2001) 131.
- [3] D. Weaire, S. Hutzler, *The Physics of Foams*, Clarendon Press, Oxford, 1999.
- [4] J. Stavans, *Rep. Prog. Phys.* 56 (1993) 733.
- [5] H. Caps, N. Vandewalle, G. Broze, *Phys. Rev. E* 73 (2006) 065301(R).
- [6] H. Caps, N. Vandewalle, G. Broze, G. Zocchi, *Appl. Phys. Lett.* 90 (2007) 214101.
- [7] A. Tufaile, J.C. Sartorelli, *Phys. Lett. A* 275 (2000) 211.
- [8] E.A. Jackson, *Perspectives of Nonlinear Dynamics*, Cambridge Univ. Press, New York, 1995.
- [9] T.M. Antonsen, A. Namenson, E. Ott, J.C. Sommerer, *Phys. Rev. Lett.* 75 (1995) 3438.
- [10] J. Argyris, G. Faust, M. Haase, *An Exploration of Chaos*, North-Holland, Amsterdam, 1994.
- [11] I. Procaccia, H.G. Schuster, *Phys. Rev. A* 28 (1983) 1210.